Effects of Solvent and Structural Dynamics on Electron Transfer Reactions of 4-Aminonaphthalene-1,8-dicarboximide Donor−Acceptor Molecules in Nematic Liquid Crystals and Isotropic Solvents

Louise E. Sinks and Michael R. Wasielewski*

Department of Chemistry and Center for Nanofabrication and Molecular Self-Assembly, Northwestern University, Evanston, Illinois 60208-3113

Received: August 7, 2002; In Final Form: November 18, 2002

Photoinduced charge separation and thermal charge recombination reactions in a series of structurally related donor−acceptor molecules based on the 4-(*N*-pyrrolidinyl)naphthalene-1,8-dicarboximide (5ANI) and 4-(*N*-piperidinyl)naphthalene-1,8-dicarboximide (6ANI) chromophores were studied in the nematic liquid crystals 4-cyano-4′-(*n*-pentyl)biphenyl (5CB) and *N*-(4′-methoxybenzylidene)-4-(*n*-butyl)aniline (MBBA) as well as in the isotropic solvents pyridine, 2-methyltetrahydrofuran, and pentyl propionate over a temperature range of 293−353 K. The photoexcited 5ANI and 6ANI chromophores donate an electron to pyromellitimide (PI), which is attached to the donors via a N−N single bond between their imide groups to give 5ANI−PI and 6ANI−PI, respectively. The photoexcited 6ANI chromophore also accepts electrons from *p*-methoxyaniline, which is attached to the 4-position of the naphthalene-1,8-dicarboximide as a *N*′-(4′-methoxyphenyl)piperazinyl substituent to give MeOAn−6ANI. Attachment of a secondary PI acceptor to MeOAn−6ANI via an imide−imide N−N single bond yields MeOAn−6ANI−PI. Photoinduced charge separation to form $MeOAn^{+}$−$6ANI^{-}$−PI is followed by thermal electron transfer to produce $MeOAn^{+}$−6ANI−PI^{-}. The charge recombination reactions in all three molecules have negative activation energies in the three isotropic Debye solvents pyridine, methyltetrahydrofuran, and pentyl propionate. This is a result of non-Condon behavior due to the internal rotational dynamics of the five- and six-membered cyclic amines about the C−N bond joining them to the naphthalene ring in 5ANI−PI, 6ANI−PI, and MeOAn−6ANI−PI on the time scale of the charge recombination reaction. This effect is not observed in 5CB and MBBA, in which slower solvent motions are strongly coupled to the electron transfer process as indicated by the fact that the electron transfer reaction rates were solvent-controlled in the liquid crystals.

Introduction

Photoinduced electron transfer is widely studied with regard to its potential applications in molecular electronics[1−4] and solar energy harvesting,[5] as well as for developing a basic understanding of redox proteins.[6−9] To rationally design a molecule-based device, it is critical to understand the role of the surrounding environment on electron transfer. Many previous studies have focused on the role of solvent in electron transfer processes,[10−17] and several excellent reviews are available.[18−21] Liquid crystals (LCs) have been studied extensively due to their applications in display technology.[22] The one-dimensional, threadlike order of nematic LCs provides an intriguing environment in which to study photoinduced electron transfer. This order provides a means of controlling electron transfer rates as well as providing insights into the mechanisms of electron transfer reactions. Nevertheless, relatively few photoinduced electron transfer reactions have been studied in LCs.[23−33] Recent examples include studies on the effects of order on the photophysical properties of 4-alkyl-*N*-(*p*-cyanophenyl) piperidines,[26] creation of photovoltaic cells from liquid crystalline porphyrins[23] and perylenediimides,[32,34] photoconduction in discotic LCs,[25,33] and time-resolved electron paramagnetic resonance measurements of photoinduced electron transfer in photosynthetic model systems dissolved in nematic LCs.[24,27,30] Studies of electron transfer reactions in LCs provide a conceptual bridge between experimental results obtained in isotropic solutions and those obtained in more ordered environments such as surfaces, monolayers, macromolecular ensembles, and crystals. In all of these cases, the "solvent" has an ordered structure that could have a critical impact on electron transfer processes. Understanding how molecular order impacts electron transfer is vitally important to developing technologies based on this process.

Solvent effects on electron transfer reactions are usually categorized as static or dynamic. Static solvent effects are usually described by a structureless dielectric bath, e.g., the Born dielectric continuum model, and are incorporated into theoretical electron transfer models via the static dielectric constant of the medium. The Marcus expression for the rate of a nonadiabatic electron transfer reaction is given by[35,36]

$$k_{ET} = \frac{2\pi {V_{DA}}^2 \exp(-\Delta G^*/k_B T)}{\hbar\sqrt{4\pi\lambda k_b T}} \qquad (1)$$

where V_{DA} is the electronic coupling matrix element, $\Delta G^* = (\Delta G + \lambda)^2/4\lambda$ is the activation energy for electron transfer, ΔG is the free energy of reaction, and λ is the total reorganization energy. The total reorganization energy is the sum of two components: the internal reorganization energy of the donor and acceptor, λ_I and the solvent reorganization energy, λ_S. Using the dielectric continuum model, Marcus has shown that λ_S can be estimated using[35,36]

10.1021/jp021833+ CCC: $25.00
Published on Web 01/07/2003

$$\lambda_s = e^2\left(\frac{1}{2r_1} + \frac{1}{2r_2} - \frac{1}{2r_{12}}\right)\left(\frac{1}{\epsilon_0} - \frac{1}{\epsilon_s}\right) \quad (2)$$

where r_1 and r_2 are the ionic radii, r_{12} is the ion pair distance, e is the charge of the electron, ϵ_S is the static dielectric constant of the solvent, and ϵ_0 is the high-frequency dielectric constant of the solvent. Jortner modified eq 1 to include the quantum mechanical nature of the internal vibrational modes of the donor and acceptor that couple to the electron transfer:[37]

$$k_{ET} = \frac{2\pi V_{DA}{}^2}{\hbar\sqrt{4\pi\lambda_s k_B T}} \sum_{m=0}^{\infty} e^{-S}\frac{S^m}{m!} e^{-[(\Delta G+\lambda_S+m\hbar\omega)^2/4\lambda_S k_B T]} \quad (3)$$

where $S = \lambda_I/\hbar\omega$, ω is a characteristic intramolecular vibrational frequency coupled to the electron transfer reaction, and ΔG is the free energy of the reaction. Once again, eq 2 is typically used to evaluate λ_S in eq 3.

Dynamic solvent effects on electron transfer reactions occur when solvent motions are slow relative to the movement of charge.[21] When these slow solvent motions, or dielectric friction, are strongly coupled to the electron transfer reaction, the reaction becomes adiabatic. For simple Debye solvents, the dynamics of solvent relaxation have a single exponential component characterized by the longitudinal relaxation time, τ_L. For a non-Debye solvent, several relaxation processes occur, and it is difficult to determine an appropriate value of τ_L from the complex dynamics.[21] If τ_L can be measured, or an appropriate distribution of values determined, nonadiabatic electron transfer theory can be modified by defining the adiabaticity parameter κ:[10]

$$\kappa = \frac{4\pi V_{DA}{}^2\tau_L}{\lambda\hbar} \quad (4)$$

where all other terms are given above. The adiabatic electron transfer rate constant, k_{AD}, can then be obtained from

$$k_{AD} = \frac{1}{1+\kappa}\cdot k_{ET} \quad (5)$$

where k_{ET} is the nonadiabatic electron transfer rate constant previously defined in eqs 1 and 3. Equation 5 has been applied to a variety of solvent systems[10] but not to LCs.

Recent work by Deeg and co-workers[38] on nematic LCs has shown that even at temperatures above the nematic to isotropic (N−I) phase transition, small ordered domains (pseudo-domains) exist. This regime is experimentally useful because optical experiments are difficult in the nematic phase of an LC due its highly scattering nature. Above the N−I phase transition, the LC is optically clear, yet significant nematic order remains. Ordered domains persist for 30−40° above the phase transition and decrease in size from approximately 20 molecular lengths to 3 molecular lengths. Unlike simple solvents, the solvent dynamics of nematic LCs are generally nonhydrodynamic. Deeg and co-workers studied the motions of 4-cyano-4′-(*n*-pentyl)-biphenyl (5CB) and found two main types of solvent relaxation, namely, a slow collective domain reorientation and a fast intradomain reordering. The collective domain reorientation, τ_{ro}, takes place on the nanosecond scale and can be modeled with the Landau−de Gennes modification of hydrodynamic theory,[38,39] as shown in eq 6

$$\tau_{ro} = \frac{e^{E_a/k_B T}}{c(T - T^*)} \quad (6)$$

Here, E_a is the activation energy for the shear viscosity of the LC,[40,41] T^* is a temperature 1−2° below the N−I phase transition (T_{NI} = 308.2 K for 5CB), and c is a fitting parameter. The faster intradomain reordering events occur on the 1−300 ps time scale and are temperature-independent for T < 343 K. Above 343 K, where no domains remain, the relaxation processes are coupled to the viscosity and show a normal hydrodynamic temperature dependence. Studies performed on *N*-(4-methoxybenzylidene)-4′-(*n*-butyl)aniline (MBBA) found similar behavior.[42]

Domain reordering can be used to control photoinduced charge separation and thermal charge recombination rates in covalently linked donor−acceptor systems. Our previous work investigated photoinduced electron transfer in a dyad consisting of a 4-(*N*-pyrrolidinyl)naphthalene-1,8-carboximide (5ANI) donor covalently attached to a pyromellitimide (PI) acceptor in 5CB and MBBA.[29,31] The charge separation reaction ^{1*}5ANI−PI → 5ANI$^+$−PI$^-$ in 5CB is nonadiabatic and obeys eq 1, while the charge recombination is adiabatic. The charge recombination time constants are proportional to the longitudinal dielectric relaxation time (τ_L) of the solvent, which correlates with the viscosity of the solvent.[21] The Landau−de Gennes theory shows that the collective domain reorientation is also coupled to the viscosity. Although τ_L and τ_{ro} are not the same, they are related, and the charge recombination times can be modeled using eq 6. When 5ANI−PI is dissolved in MBBA, the opposite effect is found, i.e., the charge separation is adiabatic, and the charge recombination is nonadiabatic. We found that these results are consistent with the alignment of 5ANI−PI along the pseudo-domain director of the LC. For example, 5CB possesses a large, positive dielectric anisotropy, where $\epsilon_{||} = 18$, $\epsilon_\perp = 6$, $\Delta\epsilon = 12$, and $\langle\epsilon\rangle = 10.5$, so that rapid rotation of 5CB about its long axis results in rapid motion of its dipole component along the perpendicular axis. This motion is fast enough to permit nonadiabatic charge separation within 5ANI−PI. On the other hand, rotation of the long axis of 5CB away from the director is relatively slow, so that electron transfer reactions coupled to that motion are adiabatic. Because the dielectric anisotropy of MBBA is negative, where $\epsilon_{||} = 4.7$, $\epsilon_\perp = 5.4$, $\Delta\epsilon = -0.7$, and $\langle\epsilon\rangle = 5.2$, the adiabaticities of the charge separation and recombination reactions for 5ANI−PI in MBBA are reversed relative to those in 5CB.

The work described here compares photoinduced charge separation and thermal charge recombination reactions in a series of structurally related donor−acceptor molecules based on the 5ANI and 4-(*N*-piperidinyl)-naphthalene-1,8-dicarboximide (6ANI) chromophores in 5CB and MBBA as well as in the isotropic solvents pyridine, 2-methyltetrahydrofuran, and pentyl propionate over a temperature range of 293−353 K. The photoexcited 5ANI and 6ANI chromophores donate electrons to PI, which is attached to the donors via a N−N single bond between their imide groups to give 5ANI−PI and 6ANI−PI, respectively (Chart 1). The photoexcited 6ANI chromophore also accepts electrons from *p*-methoxyaniline, which is attached to the 4-position of the naphthalene-1,8-dicarboximide as an *N*′-(4′-methoxyphenyl)piperazinyl substituent to give MeOAn−6ANI. Attachment of a secondary PI acceptor to MeOAn−6ANI via an imide−imide N−N single bond yields MeOAn−6ANI−PI (Chart 1). Charge separation within MeOAn−6ANI−PI occurs in the sequence ^{1*}MeOAn−6ANI−PI → MeOAn$^+$−6ANI$^-$−PI → MeOAn$^+$−6ANI−PI$^-$, a mechanism which is similar to that observed for analogous compounds having a naphthalene-1,4:5,8-bis(dicarboximide) acceptor.[43] The work presented here focuses on the influence of both solvent dynamics and internal

CHART 1

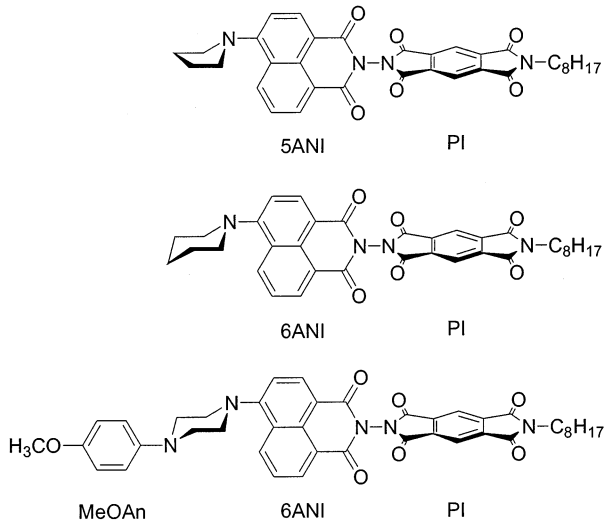

rotational dynamics within 5ANI and 6ANI on the electron transfer reactions involving these chromophores.

Experimental Section

Femtosecond transient absorption measurements were made using a regeneratively amplified titanium sapphire laser system operating at a 2 kHz repetition rate.[44] The frequency-doubled output from the laser was used to provide 420 nm, 120 fs pulses for excitation. A white light continuum probe pulse was generated by focusing the 840 nm fundamental into a 1 mm sapphire disk. Cuvettes with a dual 2/10 mm path length were used to optimize thermal contact to the thermostated cell holder (Quantum Northwest Flash 100). The samples were allowed to equilibrate for 5 min after reaching a particular temperature, T, and were held at $T \pm 0.02$ K. The samples were irradiated with 0.5−1.0 μJ per pulse focused to a 200 μm spot. The sample optical path length was 2 mm, and its optical density at the excitation wavelength was typically 0.3−0.5. The samples were stirred during the experiment using a wire stirrer to prevent thermal lensing and sample degradation. The total instrument response for the pump−probe experiments was 150 fs. Time-resolved absorption changes were obtained at a variety of temperatures between 293 and 353 K. The temperature range was dictated by the phase transition temperatures of 5CB and MBBA. Transient absorption kinetics were fit to a sum of exponentials with a Gaussian instrument function using Levenberg−Marquardt least-squares fitting. Measurements were generally repeated three times, and the resulting time constants were averaged. The deviation from the mean was generally no worse than ±10%. Steady state absorption spectra were obtained using a Shimadzu 1601 UV/vis spectrophotometer.

All solvents and LCs were purchased from Aldrich. Pentyl propionate (99.7% anhydrous), pyridine, and MBBA were used as provided. The 5CB was stored in a desiccator and used as provided. 2-Methyltetrahydrofuran (spectroscopic grade) was distilled over sodium and benzophenone and stored over sieves in a drybox until use. Immediately before use, the MTHF was additionally purified over a basic alumina column. The syntheses of 5ANI−PI and 6ANI−PI were described previously,[45,46] while that of MeOAn−6ANI−PI is described in the Supporting Information.

Results

Overview. Electron transfer theory assumes the Condon approximation, i.e., the electronic coupling matrix element V does not change on the time scale of the electron transfer reaction. We have shown previously that structural changes that modulate V on a time scale comparable to electron transfer can strongly influence the rate of the reaction.[47] It is possible that this non-Condon behavior can occur in 5ANI−PI, 6ANI−PI, and MeOAn−6ANI−PI. Changes in V may result from the internal rotational dynamics of the five- and six-membered cyclic amines about the C−N bond joining them to the naphthalene rings. In this study, we compare the results for 5ANI−PI, having the less sterically demanding five-membered ring, to those of the two 6ANI-containing molecules with their more sterically demanding six-membered rings.

The role of the solvent was probed by varying the static dielectric constant, as well as changing the nature of the solvent from simple Debye solvents characterized by a single longitudinal relaxation time, τ_L, such as MTHF and pyridine, to solvents with multiple relaxation times such as 5CB and MBBA. The longitudinal relaxation time is related to the Debye relaxation time τ_D of the solvent by $\tau_L = (\epsilon_o/\epsilon_S)\cdot\tau_D$ where ϵ_o and ϵ_S are the high-frequency and static dielectric constants, respectively, of the solvent. The Debye relaxation time of the solvent is related to the viscosity of the solvent, η, by $\tau_D = 4\pi\eta r^3/k_BT$, where r is the radius of the solvent and the other variables are defined above. The measured relaxation times for MTHF and pyridine, $\tau_L = 1.1$ ps[48] and $\tau_L \sim 0.8$ ps,[49] respectively, are fast relative to both charge separation and recombination in all of the molecules studied here, so that there should be no dynamic solvent control of these reactions. Solvents that meet these criteria, i.e., fast Debye relaxation relative to the electron transfer rate, are called "simple" in this paper to distinguish them from solvents with more complex relaxation processes. Pentyl propionate was chosen for study because it has a static dielectric constant close to $\langle\epsilon\rangle$ of MBBA and $\epsilon_\perp$ of 5CB. The value of τ_L for pentyl propionate has not been measured but should be similar to that of other alkyl esters, which exhibit Debye behavior.[11] Thus, τ_L can be estimated from its viscosity (η = 0.73 cP),[50] its radius (r = 4 Å), and its dielectric constants (ϵ_o = 1.98 and ϵ_S = 4.7)[51] using the expressions given above to yield $\tau_L \cong 5$ ps. 5CB and MBBA exhibit solvent dynamics on several different time scales that are related to motions of the LCs within the pseudo-domains as well as motions of the domains themselves.[38] On the other hand, two studies on the solvation dynamics of LCs have indicated that the relevant relaxation pathways are hydrodynamic and that the probe molecules are not embedded in the pseudo-domains but remain in disordered regions between the pseudo-domains.[52,53]

Transient Absorption Spectroscopy. The optical absorption spectrum of the radical anion of PI is very distinct, having a sharp absorption at approximately 700 nm ($\epsilon \approx 27\,000$).[45,54] This feature is clearly seen in the time-resolved absorption spectra of 5ANI−PI, 6ANI−PI, and MeOAn−6ANI−PI in 5CB. Spectra for the latter two molecules are shown in Figures 1 and 2, respectively, while that for 5ANI−PI was reported previously.[29,45] In addition, the MeOAn−6ANI−PI triad shows an additional broad absorption band centered at 550 nm at early times, which is assigned to $MeOAn^+-6ANI^-$.[43] In the triad, two sequential electron transfer events occur, ^{1*}MeOAn−6ANI−PI → $MeOAn^+-6ANI^--PI$ → $MeOAn^+-6ANI-PI^-$, so that both radical anions appear sequentially in the transient absorption spectra. For all three molecules, the time constants for charge separation and recombination at 317 K are obtained at the peak of the PI^- absorption and are summarized in Table 1. This temperature was chosen since it is the lowest temperature at which all of the solvents studied here are nonscattering and

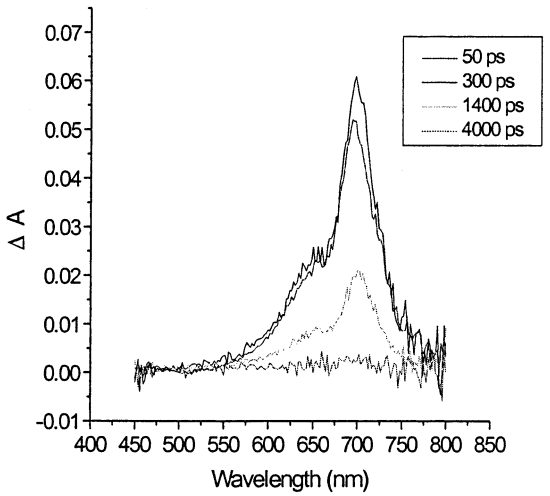

Figure 1. Time-resolved spectra of 6ANI−PI in 5CB at 317 K showing the characteristic PI^- absorption at 700 nm at the indicated times.

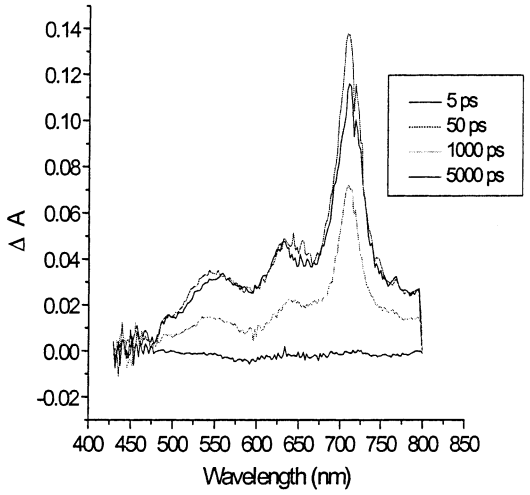

Figure 2. Time-resolved spectra of MeOAn−6ANI−PI in 5CB at 317 K showing the characteristic PI^- absorption at 700 nm and the broad absorption feature of $MeOAn^+-6ANI^-$ at 550 nm at the indicated times.

TABLE 1: Comparison of Electron Transfer Time Constants (ps) at 317−318 K

	pyridine	MTHF	PP	MBBA	5CB
charge separation					
6ANI−PI	5.2	11.0	16.4	11.9	231.1
5ANI−PI	2. 9[a]	4.7	8.9	230[a]	276.2
$MeOAn^+-6ANI-PI^-$	2.4	3.0	4.8	90.7	210.8
charge recombination					
6ANI−PI	34.6	233.6	451.3	898	597.1
5ANI−PI	31.7	244.8	414.7	615*	477.8
MeOAn−6ANI−PI	84.3	360.3	757.0	1288	463.7

[a] Data from refs 29 and 31 at 321.25 K.

all subsequent discussions of specific time constants refer to this temperature, unless otherwise noted. The charge separation and recombination time constants as a function of temperature are plotted in Figures 3−8.

The charge separation time constants, τ_{CS}, for all three molecules decrease modestly with increasing polarity for pentyl propionate ($\epsilon = 4.7$),[51] MTHF ($\epsilon = 6.9$), and pyridine ($\epsilon = 13.2$) (Table 1). The similarity of the data in MTHF and pentyl propionate confirms that the solvent dynamics of pentyl propionate have little or no effect on the electron transfer, so that pentyl propionate can be treated as a simple solvent. The

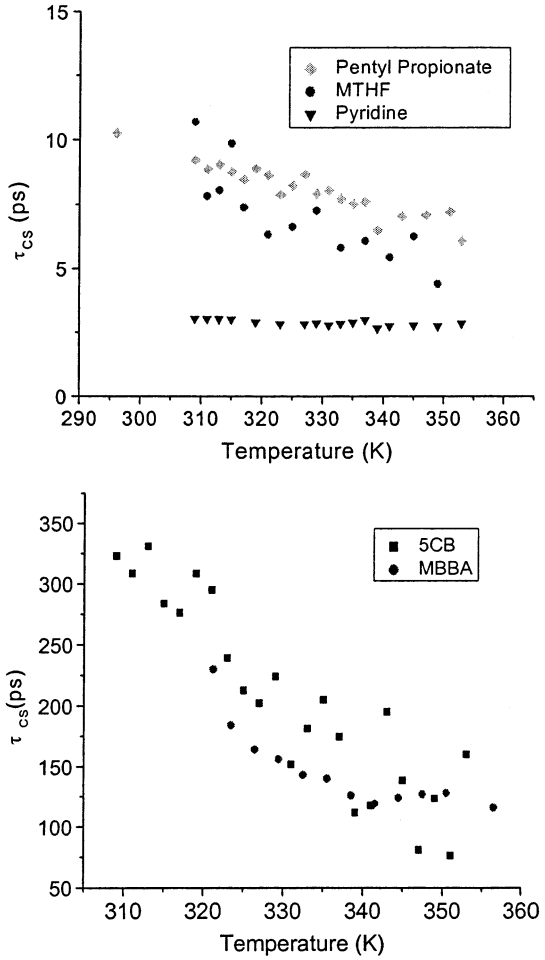

Figure 3. Solvent dependence of charge separation time constants for 5ANI−PI in various solvents. Data in MBBA are taken from ref 31.

time constants for 6ANI−PI are about twice as long as those for 5ANI−PI in the three simple solvents. The time constants for the charge shift reaction $MeOAn^+-6ANI^-−PI \rightarrow MeOAn^+-6ANI^-−PI$ are on same order of magnitude as those for the charge separation in 5ANI−PI and 6ANI−PI. In 5CB, τ_{CS} for all three molecules increases dramatically as compared to those obtained in the lowest polarity solvent, pentyl propionate. The charge separation time constant, τ_{CS}, of 5ANI−PI increases by a factor of 31, from 8.9 to 276 ps, while the τ_{CS} of 6ANI−PI increases from 16.4 to 231 ps, a 14-fold difference. The most dramatic increase in τ_{CS} occurs for the charge shift reaction $MeOAn^+-6ANI^-−PI \rightarrow MeOAn^+-6ANI-PI^-$, which is 44 times slower in 5CB, $\tau_{CS} = 210$ ps, as compared to $\tau_{CS} = 4.8$ ps in pentyl propionate. Similar effects are observed in MBBA where τ_{CS} for 5ANI−PI and MeOAn−6ANI−PI, respectively, are 25- and 20-fold longer than in pentyl propionate. However, 6ANI−PI is the exception with τ_{CS} in MBBA being comparable to that in pentyl propionate. Again, it should be emphasized that the rate ratios discussed here are specific to 317 K and that the differences diminish somewhat at higher temperatures due to the highly activated nature of electron transfer reactions in the LCs, which causes the electron transfer rates to fall off more sharply in the LCs than in the simple solvents. However, the trends appear across all of the temperatures explored here. For all three molecules, the charge separation reaction is slower in 5CB than MBBA, while charge separation within 6ANI−PI in both 5CB and MBBA is the least sensitive to the LC environment, which points to the importance of variations in the D−A structure within these systems.

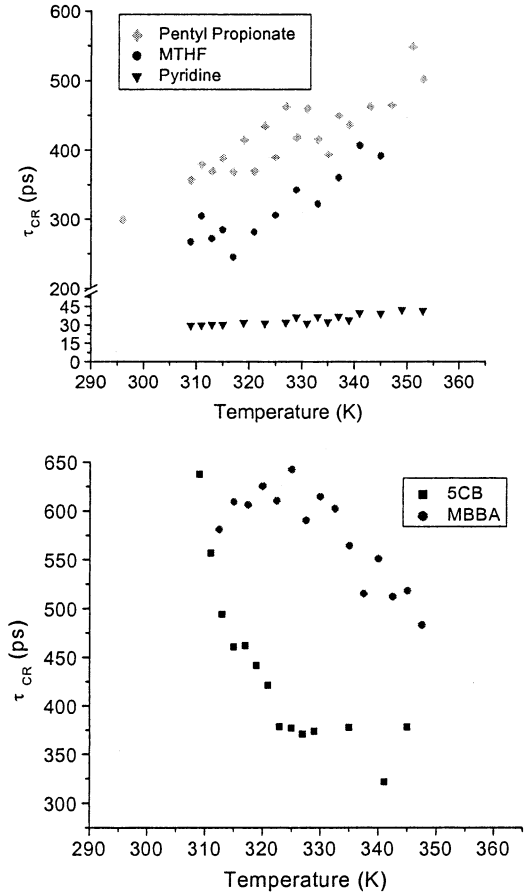

Figure 4. Solvent dependence of charge recombination time constants for 5ANI−PI in various solvents. Data in MBBA are taken from ref 31.

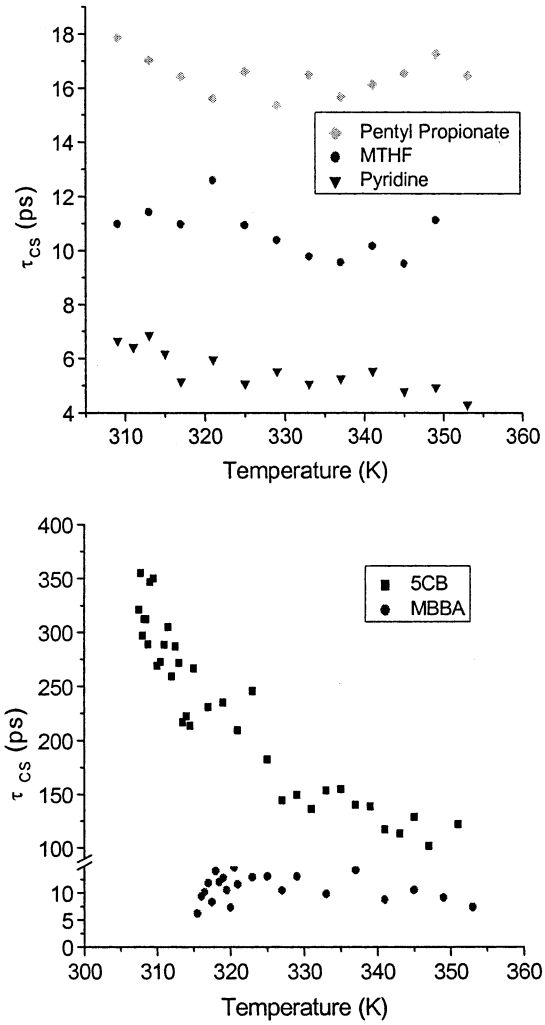

Figure 5. Solvent dependence of charge separation time constants for 6ANI−PI in various solvents.

Figures 3, 5, and 7 show the temperature dependence of τ_{CS} for 5ANI−PI, 6ANI−PI, and MeOAn−6ANI−PI in the various solvents. Activation barriers for charge separation are obtained from a plot of $\ln(k_{CS}T^{1/2})$ vs $1/T$ (shown in the Supporting Information) and are summarized in Table 2. The process is strongly activated in the LCs but only weakly activated in the simple solvents.

The charge recombination time constants, τ_{CR}, at 317 K also decrease with increasing solvent polarity for the simple solvents (Table 1). However, the difference in τ_{CR} between low polarity solvents and the LCs is not as pronounced as the differences observed for τ_{CS}. For all three molecules, τ_{CR} in both 5CB and MBBA is on the same order of magnitude as that in pentyl propionate. In MeOAn−6ANI−PI, τ_{CR} is longer in pentyl propionate than in 5CB. Again, it is critical to note that these results are specific to 317 K. The charge recombination data display unusual temperature effects (see below), and the time constant vs temperature curves for different solvents cross. At the temperatures lower and higher than 317 K, the curves diverge, and the τ_{CR} ratios change. The similarities of the values of τ_{CR} at 317 K are due to the temperature dependence curves crossing near this point and are not a trend across all temperatures.

Figures 4, 6, and 8 show the temperature dependence of τ_{CR} for 5ANI−PI, 6ANI−PI, and MeOAn−6ANI−PI in the various solvents. Activation energies for charge recombination are obtained from a plot of $\ln(k_{CS}T^{1/2})$ vs $1/T$ (shown in the Supporting Information) and are summarized in Table 3. The charge recombination is strongly activated in 5CB for all three molecules but is less so in MBBA. Surprisingly, most of the activation energies for charge recombination are negative in the simple solvents. In addition, the temperature dependence of charge recombination for $5ANI^+-PI^-$ in 5CB shows Landau−de Gennes behavior as the temperature approaches the N−I phase transition (Figure 4). Again, charge recombination within $6ANI^+-PI^-$ is strongly activated in 5CB and moderately activated in MBBA. However, Landau−de Gennes behavior for $6ANI^+-PI^-$ in 5CB, Figure 6, is much less apparent than that observed for $5ANI^+-PI^-$. The activation barriers for charge recombination within $6ANI^+-PI^-$ in the simple solvents again are negative and are larger than those observed for 5ANI−PI. For MeOAn−6ANI−PI, the thermal charge shift reaction $MeOAn^+-6ANI^--PI \rightarrow MeOAn^+-6ANI-PI^-$ also exhibits negative activation energies in pentyl propionate and MTHF (Table 3).

Discussion

Structural Dynamics Coupled to Electron Transfer. The two principal degrees of freedom within 5ANI−PI, 6ANI−PI, and MeOAn−6ANI−PI that may lead to structural variations among these molecules and could influence their electron transfer reactions are rotation of the cyclic amine about the C−N bond joining it to the naphthalene ring and rotation of naphthalene-1,8-dicarboximide about the N−N bond joining it to PI. The energy-minimized ground state structures of 5ANI−PI and 6ANI−PI were calculated using the AM1 method.[55]

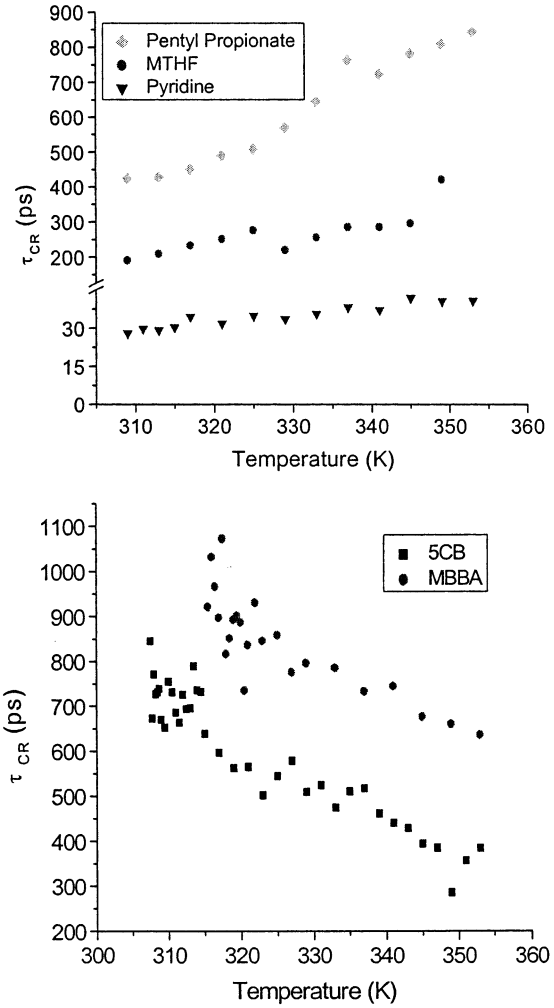

Figure 6. Solvent dependence of charge recombination time constants for 6ANI−PI in various solvents.

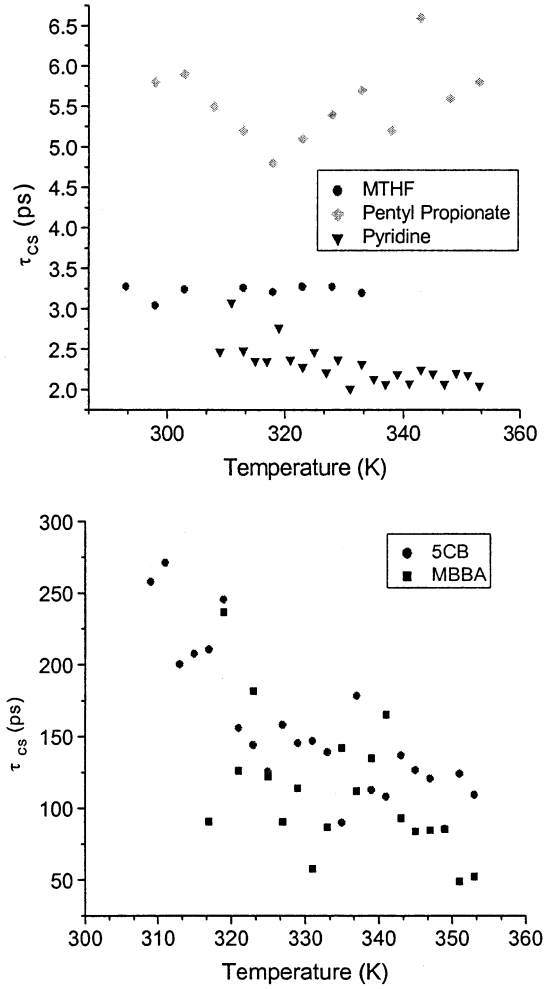

Figure 7. Solvent dependence of charge separation time constants for MeOAn−6ANI−PI in various solvents.

These structures show that the dihedral angle between the imide groups of 5ANI and 6ANI and that of the attached PI is fixed at about 90° presumably by the significant steric interactions of the four carbonyl groups surrounding the N−N bond. The calculated dihedral angles, θ, between the nitrogen lone pair of the cyclic amines in the 5ANI and 6ANI chromophores and the π system of the naphthalene-1,8-dicarboximide are 18 and 49°, respectively. Saha and co-workers[56] have recently reported the crystal structures of the 5ANI and 6ANI chromophores, which show that $\theta = 0°$ for 5ANI and $\theta = 40°$ for 6ANI, so that 5ANI has increased overlap between the ring nitrogen lone pair and the naphthalene π system as compared to 6ANI. This large difference in dihedral angle is most likely due to the increased steric hindrance in the six-membered ring, as its ring hydrogens interact with the peri hydrogens of the naphthalene. The trend in the values of θ obtained from the calculations agrees well with that obtained from the crystal structures.

Excitation of 5ANI or 6ANI to their lowest excited singlet CT states places positive charge density on the nitrogen atom at the 4-position and negative charge density on the naphthalene-1,8-dicarboximide.[43,56] Following formation of the ^{1*}5ANI and ^{1*}6ANI CT states and subsequent electron transfer to form $5ANI^+$ and $6ANI^+$, it is possible that rotation of the cyclic amine occurs to stabilize the positive charge as it develops on the amine nitrogen resulting in a significant decrease in θ. To examine this idea, the energy-minimized structures of $5ANI^+$ and $6ANI^+$ were calculated using the unrestricted Hartree−Fock AM1 method. These structures show that θ is 6 and 28° in $5ANI^+$ and $6ANI^+$, respectively. Thus, it is likely that rotation of the cyclic amine stabilizes the ^{1*}5ANI and ^{1*}6ANI CT states, as well as $5ANI^+$ and $6ANI^+$, which produce both a structure and a charge distribution that has a more favorable electronic coupling V, for both charge separation and recombination. However, the cyclic amine in 5ANI needs to rotate over a much smaller dihedral angle than does that of 6ANI.

TABLE 2: ΔG^* (eV) for Charge Separation

	5ANI−PI	6ANI−PI	MeOAn−6ANI−PI (charge shift)
5CB	0.28	0.21	0.21
MBBA	0.17[a]	0.12	0.21
pyridine	0.04	0.09	0.06
MTHF	0.07	0.05	0.02
PP	0.09	0.02	0.01

[a] Data from refs 29 and 31.

Greenfield et al.[43] showed that the lowest excited singlet state of 6ANI has about 70% CT character. They also showed that the resulting solvatochromism of ^{1*}6ANI can be used to estimate with reasonable accuracy the free energy of solvation for charge separation within a particular solvent. As a consequence, electron transfer reactions to or from ^{1*}6ANI can be treated as charge shift reactions for the purpose of determining the free energies of these electron transfers. The results of our electronic structure calculations and the crystal structures of Saha et al.[56] strongly suggest that the CT character within ^{1*}5ANI should be even larger than that of ^{1*}6ANI, so that the Greenfield method for

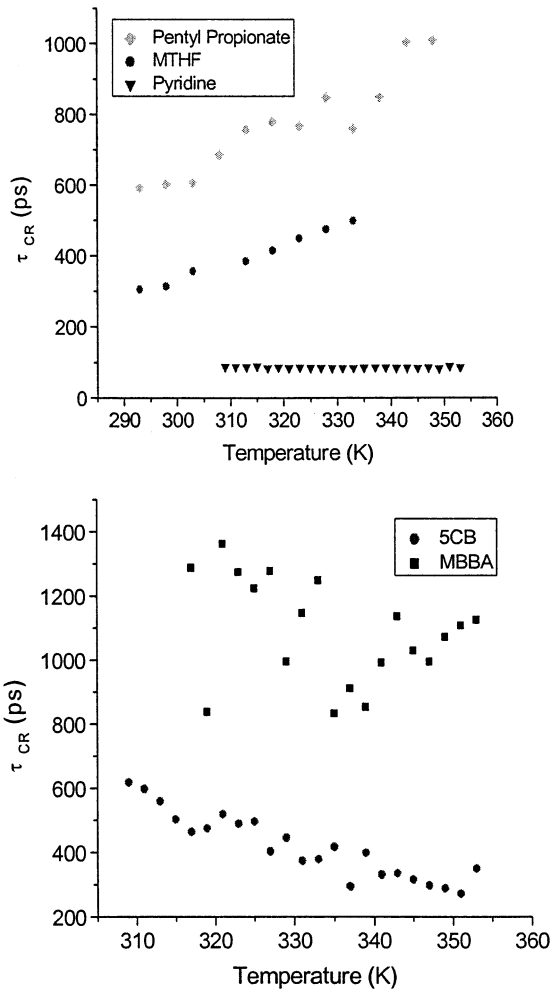

Figure 8. Solvent dependence of charge recombination time constants for MeOAn−6ANI−PI in various solvents.

TABLE 3: ΔG^* (eV) for Charge Recombination

	5ANI−PI	6ANI−PI	MeOAn−6ANI−PI (charge shift)
5CB	0.12	0.17	0.17
MBBA	0.08[a]	0.11	0.05
pyridine	−0.06	−0.06	0.02
MTHF	−0.09	−0.12	−0.11
PP	−0.06	−0.15	−0.07

[a] Data from refs 29 and 31.

determining free energies of reaction should also be valid for compounds containing 5ANI. The free energies of charge separation for all three molecules were calculated using this simple method (Table 4) and suggest that the charge separation rates for 5ANI−PI and 6ANI−PI should be approximately the same. However, the rate of charge separation for 5ANI−PI is about twice as fast than that for 6ANI−PI in the simple solvents, indicating that the electronic coupling V between ^{1*}5ANI and PI is somewhat larger than that between ^{1*}6ANI and PI. Given that our experimental charge separation time constants are longer than τ_L and that normal Arrhenius temperature dependence is observed for the charge separation, it is unlikely that rotation of the cyclic amine plays an important role in the overall charge separation reaction within the simple Debye solvents.

The negative activation energies observed for the charge recombination reactions suggest that rotation of the cyclic amine may be coupled to the recombination process. As the temperature increases, the cyclic amine most likely rotates away from the stable energy minimum of the radical cation, diminishing the overall electronic coupling and decreasing the electron transfer rate. The larger rotational barrier due to steric hindrance of the cyclic amine in 6ANI, as compared to that of 5ANI, leads one to predict that the magnitude of ΔG^* should be larger for 6ANI than for 5ANI, as is observed experimentally.

TABLE 4: Free Energies of Reaction[a]

	pyridine	MTHF	PP	MBBA	5CB
		ΔG_{CS} (in eV)			
6ANI−PI	−0.56	−0.50	−0.44	−0.46	−0.54
5ANI−PI	−0.56	−0.50	−0.44	−0.46	−0.54
MeOAn−6ANI−PI (charge shift)	−0.58	−0.54	−0.50	−0.51	−0.57
		ΔG_{CR} (in eV)			
6ANI−PI	−2.24	−2.30	−2.36	−2.34	−2.26
5ANI−PI	−2.09	−2.15	−2.21	−2.09	−2.01
MeOAn−6ANI−PI	−1.90	−1.94	−1.98	−1.97	−1.91

[a] See ref 43 for method of calculation and ref 45 for values used in the calculation.

It is also possible to obtain an overall negative activation barrier for the electron transfer reaction if it proceeds through an intermediate. The appearance of the negative activation barrier depends on the relative magnitudes of the activation energies for the formation and decay of the intermediate. This intermediate could be a rotational isomer of the radical cation that forms prior to the charge recombination. While it is difficult to rule out such a process, our data provide no direct evidence for an intermediate. In our earlier work on the breakdown of the Condon approximation in electron transfer reactions, we were able to show that under favorable circumstances it is possible to relate the magnitude of the negative activation barrier to the energy of a known torsional mode in the electron donor, which provides evidence for coupling the torsion to the electron transfer.[47] Unfortunately, in the present case, no such information on the frequencies of ring torsional modes in either $6ANI^+$ or $5ANI^+$ is currently available.

Previous work on a triad similar to MeOAn−6ANI−PI determined the mechanism of charge separation and charge shift but could not determine the mechanism of charge recombination.[43] The work presented here allows us to clarify the mechanism of charge recombination in this type of triad. The similarity of the ΔG^* values for charge recombination within $MeOAn^+$−6ANI−PI^- and $6ANI^+$−PI^- in all solvents suggests that the charge recombination occurs via rapid hole transfer from $MeOAn^+$ to 6ANI to form $6ANI^+$ followed by collapse of the $MeOAn-6ANI^+-PI^-$ ion pair analogous to $6ANI^+-PI^-$. The latter process is expected to be strongly temperature-dependent for reasons discussed above. If the mechanism was to collapse the $MeOAn^+-6ANI-PI^-$ ion pair via superexchange, or a stepwise process involving the $MeOAn^+-6ANI^--PI$ intermediate, both the signs and the magnitudes of the activation energies would be expected to be different. For example, the positive charge on the nitrogen atom of $MeOAn^+$ is unlikely to interact strongly with the naphthalene π system due to its distance and geometry. Moreover, a rate-limiting electron transfer from PI^- to 6ANI cannot involve a significant geometry change in 6ANI due to the very sterically crowded 6ANI−PI linkage. Because the alignment of the lone pair orbital of the nitrogen atom attached to the naphthalene is not relevant to the electron transfer from PI^- to 6ANI, the activation energy is unlikely to be negative, since the negative activation energy arises directly from the modulation of V by rotation of the piperazine ring relative to the naphthalene on a time scale similar to that for the charge recombination. Additionally, the rates of

recombination for MeOAn−6ANI−PI are on the same order of magnitude as the 6ANI−PI recombination (Table 3).

Effect of Solvent Dynamics on Electron Transfer. Our data show that in the simple Debye solvents, solvent relaxation occurs more rapidly than charge separation to form $5ANI^+-PI^-$, $6ANI^+-NI^-$, and $MeOAn^+-6ANI-PI^-$. In addition, charge recombination is most likely controlled by modulation of V due to rotation of the cyclic amine. However, the behavior of these molecules in the LC solvents is much more complex. Not only is there the possibility of non-Condon effects due to structural changes in the molecules, but the relatively slow motions of the LC are undoubtedly coupled to both the charge separation and the recombination. Given the linear, cylindrical structures of the donor−acceptor molecules, it is reasonable to assume that they reside in the pseudo-domains of the LCs, which are structurally very similar. However, two reports on the solvent dynamics of LCs raise the possibility that the probe molecules may lie in disordered regions between the pseudo-domains.[52,57] Both cases will be examined with regard to static solvent effects, dynamic solvent effects, and solvent-induced structural changes in 5ANI and 6ANI.

Equations 1−3 show that static solvent effects directly impact the free energy of reaction and thus the magnitude of the activation barrier and the electron transfer rate. The reason that the activation barrier height may be influenced by solvent relaxation times derives from the fact that τ_L is most likely a function of T, such that a plot of $\ln(kT^{1/2})$ vs $1/T$ will have a slope that not only depends on the electron transfer energetics but also will include the temperature dependence of τ_L. The average dielectric constant of 5CB ($\langle\epsilon\rangle = 10.5$) is similar to that of pyridine ($\epsilon = 13.2$), while the average dielectric constant of MBBA ($\langle\epsilon\rangle = 5.2$) is similar to those of MTHF ($\epsilon = 6.9$) and pentyl propionate ($\epsilon = 4.7$). However, the rates of both charge separation and recombination are dramatically slower in both 5CB and MBBA than in any of the simple solvents, which suggests that dynamic solvent control is responsible for the slow rates in the LCs. Equation 4 shows that the adiabaticity of an electron transfer reaction depends on both V^2 and τ_L and is more sensitive to changes in V due to its quadratic dependence. As discussed above, V should be smaller for the reaction $^{1*}6ANI-PI \rightarrow 6ANI^+-PI^-$ than the corresponding reaction $^{1*}5ANI-PI \rightarrow 5ANI^+-PI^-$, making the former reaction less adiabatic than the latter reaction. This may account for why the charge separation time constant for 6ANI−PI in MBBA is comparable to those observed in the simple Debye solvents.

If the donor−acceptor molecule is embedded in the LC pseudo-domains, the bulk dielectric constant is unlikely to be the appropriate metric of the environment experienced by the donor−acceptor molecule. Because 5CB has a large dielectric anisotropy, ΔG^* was calculated for 5ANI−PI and 6ANI−PI in 5CB using eq 3 with a set of model parameters including the anisotropic dielectric constants ($\epsilon_{||} = 18$, $\epsilon_{\perp} = 6$) and the free energies of reaction, while the electronic coupling V was varied between 5 and 200 cm^{-1} to match the experimental rate constants. For example, using a dielectric constant of six and an electronic coupling of 7 cm^{-1}, the calculated time constant for charge separation for 6ANI−PI in 5CB is $\tau_{CS} = 228$ ps at 306 K, close to the experimental value, but the calculated activation energy, $\Delta G^* = 0.01$ eV, differs substantially from the experimental value of 0.21 eV. Similar discrepancies arise if one tries to use $\epsilon_{||} = 18$ as the effective dielectric constant of 5CB. Deeg and Fayer indicate that the fast intradomain motions are temperature-independent. These solvent motions occur on a ~300 ps time scale. Using eq 5 to estimate charge separation rate constants, the predicted activation energy assuming $\tau_L = 300$ ps, $\omega = 1500$ cm^{-1}, and $\lambda_I = 0.3$ eV is on the order of 0.02 eV regardless of choice of dielectric constant ($\epsilon = 5$ or 10) or electronic coupling ($V = 50$ or 100 cm^{-1}) and gives time constants of $\tau_{CR} = 906$ ps at 306 K that are only slightly longer than the experimental time constants. Once again, the calculations yield the appropriate time constants but fail to accurately predict ΔG^*.

A relatively large activation barrier may also arise from the nematic potential, q. When an electric field is applied to a nematic LC, either by the dipolar CT excited state of the donor or by the ion pair itself, reorientation of the dipolar LC molecule is hindered by the nematic potential,[58] which has a well-known impact on the relaxation time of the LC. Additionally, the presence of the nematic potential may increase the solvent reorganization energy beyond what is predicted by eq 2. Models of the nematic potential and its effect on relaxation times both use the unitless order parameter S, which is a measure of the bulk alignment:

$$S = \frac{3\langle\cos^2\phi\rangle - 1}{2} \tag{7}$$

where ϕ is the angle between a molecule and the LC director and $\langle\cos^2\phi\rangle$ is averaged over all molecules. S ranges from 1 (perfectly aligned) to 0 (completely disordered). It is unclear what the value of the parameter should be for a molecule in a pseudo-domain where the local order is very high, but bulk order is low. Nevertheless, if the nematic potential concept can be applied to the pseudo-domains, then the relaxation time becomes temperature-dependent as well,[27] although its dependence is complex:

$$\tau_D = \frac{e^{q/kT} - 1}{q/kT} \cdot \tau_D{}^0 \tag{8}$$

Here, $\tau_D{}^0$ is the Debye relaxation in an isotropic solvent and τ_D is related to τ_L by the ratio of the static and high-frequency dielectric constants, and all other terms are defined previously. In principle, q is temperature-dependent as well, since it depends on the order parameter S, which is presumably temperature-dependent, although that relates to how S is defined within the pseudo-domains. If the concept of nematic potential is important for describing the behavior of these molecules, then the electron transfer rates in LCs at high temperatures should be similar to those in simple solvents wherein no pseudo-domain exist. This means that the activation energy for charge separation should decrease, so that electron transfer becomes temperature-independent at high temperatures, while the activation energy for charge recombination should be negative due to the modulation of V by structural changes in the donor−acceptor molecules. This is not observed for charge separation, nor for charge recombination, which leads us to explore an additional structural argument as a possible explanation for the activation energy of charge separation, since the solvent arguments fail at high temperatures.

A change in the donor−acceptor structure for molecules within the pseudo-domains assumes that the minimum energy structure of $^{1*}5ANI$ and $^{1*}6ANI$ in the LCs is different than that in the simple Debye solvents. If there is less CT character for $^{1*}5ANI$ and $^{1*}6ANI$ in the LCs, so that the electronic coupling between these excited CT states and PI is reduced, increased temperature is necessary to allow rotation of the cyclic amines into an appropriate position for electron transfer to occur. The kind of dramatic change in θ between the ground and the

excited CT state might be inhibited by inertial effects or by strong intermolecular interactions that would prevent disruption of the local LC order of the pseudo-domains. However, this type of structural effect must also explain charge recombination, so that the ring motion of $5ANI^+$ and $6ANI^+$ must be strongly temperature-dependent. However, this explanation fails in the high-temperature limit, where recombination should slow with increasing temperature as it does in the simple Debye solvents. Thus, residence of 5ANI−PI and 6ANI−PI in the pseudo-domains over the entire temperature range measured cannot explain both the observed charge separation and the recombination temperature dependencies.

If the donor−acceptor molecules reside in regions of disorder between the pseudo-domains at high temperatures, the structural arguments made in the simple solvents still apply here, since there are no unusual interactions between the D−A molecule and the nematic pseudo-domains. The solvent molecules that solvate the donor−acceptor molecules should follow standard hydrodynamic theory,[38,42,52,53,57] not Landau−de Gennes theory, and the electron transfer rates should correlate with the solvent viscosity. Because the solvent motions are temperature-dependent and show Arrhenius behavior, the experimentally measured activation energies for electron transfer are a combination of the solvent reorientational activation energy and the intrinsic electron transfer activation energy. Urban et al.[59] measured the low-frequency dielectric relaxation time of 5CB to be $\tau_L = 1.314 \times 10^{-14} \exp(33\,200/RT)$. Putting this function for τ_L into eq 5 for charge separation, setting the dielectric constant to $\epsilon = 5$ or 10, and varying the electronic coupling from 1 to 200 cm^{-1} to match the observed kinetics predicts activation energies on the order of 0.35 eV. This prediction of a strongly activated process agrees better with experiment than the very low barrier found when the donor−acceptor molecules are embedded in the pseudo-domains, although it is larger than what was experimentally determined. However, the time constants for charge separation found using this value of τ_L were on the order of tens of nanoseconds, which obviously do not match the experimental results. Studies of 5CB in *n*-hexane, where dilution prevents the formation of pseudo-domains, found relaxation processes with the same functional form and barrier height but which occur on faster time scales, 40−140 ps for the slower process and 12−24 ps for the faster process.[38] Assuming that the slower process is the relevant dielectric relaxation process, the same calculation produces charge separation times on the order of hundreds of picoseconds, which are consistent with our experimental data. The hydrodynamic model is general so that it applies to both 5CB and MBBA.[42] Only the specific values of τ_L will change, although they should be similar for MBBA and 5CB. This theory also explains the positive activation energy for the recombination process because the increase in the dielectric relaxation rate with increasing temperature can more than compensate for the decreased electronic coupling. This model applies for all temperatures, since it is independent of the pseudo-domains, so the high-temperature results should be different from the simple solvents. The consistency of this model with our experimental data over the entire temperature range measured suggests that both the charge separation and the recombination rates are solvent-controlled in the LCs and that these donor−acceptor molecules are most likely not embedded in the pseudo-domains.

In LCs, at temperatures near the N−I phase transition, the electron transfer reactions are more strongly adiabatic due to slower solvent relaxation mechanisms that are not active at higher temperatures. These additional solvent relaxation processes depend critically on the nematogenic character of the LC because τ_{CS} and τ_{CR} increase asymptotically as T_{NI} is approached. This gives the temperature dependencies of τ_{CS} in MBBA and τ_{CR} in 5CB for 5ANI−PI their characteristic Landau−de Gennes functional form. This effect is accentuated in 5ANI−PI because V is larger for both charge separation and recombination relative to 6ANI−PI, which results in an increase in the overall adiabaticity for the reactions in 5ANI−PI. Electron transfer with 6ANI−PI and MeOAn−6ANI−PI is less adiabatic and thus Landau−de Gennes behavior appears very weakly, if at all, in the corresponding temperature dependencies of the electron transfer time constants.

Conclusions

Studies on a series of structurally related donor−acceptor molecules based on the ANI chromophore show that rotational motion of the cyclic amine plays a critical role in the electron transfer process. The CT character of the excited state is directly controlled by the motion of the cyclic amine and has a clear influence on the rates of charge separation. As a consequence, the donor−acceptor dyads and triad all have negative activation barriers for charge recombination in fast relaxing Debye solvents. In the LCs, the electron transfer dynamics of the donor−acceptor dyads and triad couple very strongly to the hydrodynamic motions of the solvent for both charge separation and charge recombination. Thus, the interplay of structural changes within these molecules and solvent dynamics results in a complex dependence of the electron transfer rates on temperature. Balancing these effects may allow one to design systems in which the relatively slow solvent dynamics of the LCs can be used to promote long-lived charge-separated states of interest to photochemical conversion and storage of solar energy.

Acknowledgment. We thank Dr. Ryan T. Hayes (NU) for many helpful discussions on all aspects of this work. This work was supported by the Division of Chemical Sciences, Office of Basic Energy Sciences, U.S. Department of Energy, under Grant No. DE-FG02-99-ER14999.

Supporting Information Available: Synthesis of MeOAn−6ANI−PI and plots of $\ln(k_{CS}T^{1/2})$ vs $1/T$ and $\ln(k_{CR}T^{1/2})$ vs $1/T$ for each compound in each solvent studied. This material is available free of charge via the Internet at http://pubs.acs.org.

References and Notes

(1) Seta, P.; Bienvenue, E.; Moore, A. L.; Moore, T. A.; Gust, D. *Electrochim. Acta* **1989**, *34*, 1723−1727.

(2) Hopfield, J. J.; Onuchic, J. N.; Beratan, D. N. *Science* **1988**, *241*, 817−819.

(3) De Silva, A. P.; Gunaratne, H. Q.; McCoy, C. P. *Nature* **1993**, *364*, 42−44.

(4) Davis, W. B.; Svec, W. A.; Ratner, M. A.; Wasielewski, M. R. *Nature* **1998**, *396*, 60−63.

(5) Imahori, H.; Norieda, H.; Yamada, H.; Nishimura, Y.; Yamazaki, I.; Sakata, Y.; Fukuzumi, S. *J. Am. Chem. Soc.* **2001**, *123*, 100−110.

(6) Greenfield, S. R.; Seibert, M.; Govindjee; Wasielewski, M. R. *Chem. Phys.* **1995**, *210*, 279−295.

(7) Prasad, E.; Gopidas, K. R. *J. Am. Chem. Soc* **2000**, *123*, 1159−1165.

(8) Axup, A. W.; Albin, M.; Mayo, S. L.; Crutchley, R. J.; Gray, H. B. *J. Am. Chem. Soc.* **1988**, *110*, 435−439.

(9) Book, L. D.; Arnett, D. C.; Hu, H.; Scherer, N. F. *J. Phys. Chem. A* **1998**, *102*, 4350−4359.

(10) Heitele, H.; Michel-Beyerle, M. E. *Chem. Phys. Lett.* **1987**, *138*, 237−243.

(11) Horng, M. L.; Gardecki, J. A.; Papazyan, A.; Marconcelli, M. *J. Phys. Chem.* **1995**, *99*, 17311−17337.

(12) Jarzeba, W.; Walker, G. C.; Johnson, A. E.; Kahlow, M. A.; Barbara, P. F. *J. Phys. Chem.* **1988**, *92*, 7039−7041.
(13) Kahlow, M. A.; Jarzeba, W.; Kang, T. J.; Barbara, P. F. *J. Chem. Phys.* **1989**, *90*, 151−158.
(14) Marconcelli, M.; Fleming, G. R. *J. Chem. Phys.* **1987**, *86*, 6221−6239.
(15) McManis, G. E.; Weaver, M. J. *J. Phys. Chem.* **1989**, *90*, 912−922.
(16) Nielson, R. M.; McManis, G. E.; Weaver, M. J. *J. Phys. Chem.* **1989**, *93*, 4703−4706.
(17) Weaver, M. J.; McManis, G. E.; Jarzeba, W.; Barbara, P. F. *J. Phys. Chem.* **1990**, *94*, 1716−1719.
(18) Barbara, P. F.; Jarzeba, W. *Acc. Chem. Res.* **1988**, *21*, 195−199.
(19) Barbara, P. F.; Walker, G. C.; Smith, T. *Science* **1992**, *256*, 975−981.
(20) Maroncelli, M.; MacInnis, J.; Fleming, G. R. *Science* **1989**, *243*, 1674−1681.
(21) Weaver, M. J.; McManis, G. E., III. *Acc. Chem. Res.* **1990**, *23*, 294−300.
(22) Kahn, F. J. *Phys. Today* **1982**, *May*, 66−74.
(23) Gregg, B. A.; Fox, M. A.; Bard, A. J. *J. Phys. Chem.* **1990**, *94*, 1586−1597.
(24) Hasharoni, K.; Levanon, H.; Von Gersdorff, J.; Kurreck, H.; Moebius, K. *J. Chem. Phys.* **1993**, *98*, 2916−2926.
(25) Adam, D.; Schuhmacher, P.; Simmerer, J.; Haussling; Siemensmeyer, K.; Etzbach, K. H.; Ringsdorf, I.; Haarer, D. *Nature* **1994**, *371*, 141−143.
(26) Sheikh-Ali, B. M.; Weiss, R. G. *J. Am. Chem. Soc.* **1994**, *116*, 6111−6120.
(27) Hasharoni, K.; Levanon, H. *J. Phys. Chem.* **1995**, *99*, 4875−4878.
(28) Hasharoni, K.; Levanon, H.; Greenfield, S. R.; Gosztola, D. J.; Svec, W. A.; Wasielewski, M. R. *J. Am. Chem. Soc.* **1996**, *118*, 10228−10235.
(29) Wiederrecht, G. P.; Svec, W. A.; Wasielewski, M. R. *J. Am. Chem. Soc.* **1997**, *119*, 6199−6200.
(30) Levanon, H.; Galili, T.; Regev, A.; Wiederrecht, G. P.; Svec, W. A.; Wasielewski, M. R. *J. Am. Chem. Soc.* **1998**, *120*, 6366−6373.
(31) Wiederrecht, G. P.; Svec, W. A.; Wasielewski, M. R. *J. Phys. Chem. B* **1999**, *103*, 1386−1389.
(32) Struijk, C. W.; Sieval, A. B.; Dakhorst, J. E. J.; van Dijk, M.; Kimkes, P.; Koehorst, R. B. M.; Donker, H.; Schaafsma, T. J.; Picken, S. J.; van de Craats, A. M.; Warman, J. M.; Zuilhof, H.; Sudholter, E. J. R. *J. Am. Chem. Soc.* **2000**, *122*, 11057−11066.
(33) Schmidt-Mende, L.; Fechtenkotter, A.; Mullen, K.; Moons, E.; Friend, R. H.; MacKenzie, J. D. *Science* **2001**, *293*, 1119−1122.
(34) Gregg, B. A.; Cormier, R. A. *J. Am. Chem. Soc.* **2001**, *123*, 7959−7960.
(35) Marcus, R. A. *J. Chem. Phys.* **1956**, *24*, 966−978.
(36) Marcus, R. A.; Sutin, N. *Biochim. Biophys. Acta* **1985**, *811*, 265−322.
(37) Jortner, J. *J. Phys. Chem.* **1976**, *64*, 4860−4867.
(38) Deeg, F. W.; Greenfield, S. R.; Stankus, J. J.; Newell, V. J.; Fayer, M. D. *J. Chem. Phys.* **1990**, *93*, 3503−3514.
(39) de Gennes, P. G. *Mol. Cryst. Liq. Cryst.* **1971**, *12*, 193-214.
(40) Martinoty, P.; Candau, S.; Debeauvais, F. *Phys. Rev. Lett.* **1971**.
(41) Martinoty, P.; Kiry, F.; Nagai, S.; Candau, S. *J. Physiol.* **1977**, *38*, 159−162.
(42) Stankus, J. J.; Torre, R.; Fayer, M. D. *J. Phys. Chem.* **1993**, *97*, 9478−9487.
(43) Greenfield, S. R.; Svec, W. A.; Gosztola, D.; Wasielewski, M. R. *J. Am. Chem. Soc.* **1996**, *118*, 6767−6777.
(44) Lukas, A. S.; Miller, S. E.; Wasielewski, M. R. *J. Phys. Chem.* **2000**, *104*, 931−940.
(45) Debreczeny, M. P.; Svec, W.; Wasielewski, M. R. *New J. Chem.* **1996**, *20*, 825−828.
(46) Wiederrecht, G. P.; Svec, W. A.; Wasielewski, M. R. *J. Am. Chem. Soc.* **1999**, *121*, 7726−7727.
(47) Davis, W. B.; Ratner, M. A.; Wasielewski, M. R. *J. Am. Chem. Soc.* **2001**, *123*, 7877−7886.
(48) Gorlach, E.; Gygax, H.; Lubini, P.; Wild, U. P. *Chem. Phys.* **1995**, *194*, 185−193.
(49) Van Der Zwan, G.; Hynes, J. T. *Chem. Phys. Lett.* **1983**, *101*, 367−371.
(50) Klimova, T. F.; Guseinov, K. D.; Bairamov, N. M. *Inzh.-Fiz. Zh.* **1978**, *35*, 163−164.
(51) *CRC Handbook of Chemistry and Physics*, 81st ed.; CRC Press: Cleveland.
(52) Saielli, G.; Polimeno, A.; Nordi, P. L.; Bartolini, P.; Ricci, M.; Righini, R. *J. Chem. Soc., Faraday Trans.* **1998**, *94*, 121−128.
(53) Choi, M.; Jin, D.; Kim, H. *J. Phys. Chem. B* **1997**, *101*, 8092−8097.
(54) Gosztola, D.; Niemczyk, M. P.; Svec, W. A.; Lukas, A. S.; Wasielewski, M. R. *J. Phys. Chem. A* **2000**, *104*, 6545−6551.
(55) AM1 calculations were performed using HyperChem, Hypercube, Inc., 1115 NW 1114th Street, Gainesville, FL 32601.
(56) Saha, S.; Samanta, A. *J. Phys. Chem. A* **2002**, *106*, 4763−4771.
(57) Rau, J.; Ferrante, C.; Deeg, F. W.; Brauchle, C. *J. Phys. Chem. B* **1999**, *103*, 931−937.
(58) Martin, A. J.; Meier, G.; Saupe, A. *Symp. Faraday Soc.* **1971**, *6*, 119−133.
(59) Urban, S.; Gestblom, B.; Wurflinger, A. *Mol. Cryst. Liq. Cryst.* **1999**, *331*, 113−120.